Supplementary Information

Dual element (C-Cl) isotope approach to distinguish abiotic reactions of chlorinated methanes by Fe(0) and by Fe(II) on iron minerals at neutral and alkaline pH

Diana Rodríguez-Fernández[†], Benjamin Heckel[§], Clara Torrentó[‡], Armin Meyer[§], Martin Elsner[§], Daniel Hunkeler[‡],

Albert Soler[†], Mònica Rosell[†], Cristina Domènech[†]

†Grup MAiMA, Mineralogia Aplicada, Geoquímica i Geomicrobiologia, Departament de Mineralogia, Petrologia i Geologia Aplicada, Facultat de Ciències de la Terra, Martí Franques s/n, Universitat de Barcelona (UB), 08028 Barcelona, Spain.

§Institute of Groundwater Ecology, Helmholtz Zentrum München, 85764 Neuherberg, Germany.

*Centre for Hydrogeology and Geothermics, Université de Neuchâtel, 2000 Neuchâtel, Switzerland.

Corresponding author: Diana Rodríguez-Fernández (diana.rodriguez@ub.edu)

Total number of pages (including cover):23

Scheme: 1

Figures: 9

Tables: 3

1. Chemicals

HEPES buffer (99.5%, Sigma-Aldrich) was used to prepare the buffer at pH 7 (0.2 mM). 10 mM sodium hydroxide (NaOH, Baker) was used to prepare the buffer at pH 12. For the CF_Fe_12 and CF_CO_12 experiments, pure CF (99.5%, Fluka) was used. Pure CF (99%, Merck) was used for the CF Mag, Py and aqueous FeCl₂ experiments and corresponding controls, since they were performed in different laboratories. For all the CT experiments, pure CT (99%, Panreac) was used. A solution of 0.6 mM FeCl₂ (99.99%, purity, Sigma-Aldrich) was prepared for the CF_aq_7, CF_aq_12, CT_aq_7, CT_aq_12 and experiments with Mag and Py. Milli-sized iron (92% purity) from Gotthart Maier Metallpulver GmbH was used in the CF_Fe_12 experiments. Nano-sized iron (99%, Sigma-Aldrich) was used for the CT_Fe_7 and CT_Fe_12 experiments. 1 M acetic acid solution was prepared from glacial acetic acid (CH₃CO₂H, Sigma-Aldrich) to quenching pH 12 solution in order to avoid further CF alkaline hydrolysis in the pH 12 experiments concerning this compound.

2. Minerals and Fe(0) preparation and characterization

Natural Py and Mg crystals were obtained from sedimentary deposits in Navajún (Logroño, Spain) and from a retrograding skarn from Mina Cala (Huelva, Spain), respectively. The X-ray diffraction patterns confirmed they were Py and Mag and showed no significant evidence of any other mineral phase, although some impurities (Ca, Al, Mn in Py and Ca and Ti in Mag) were identified with scanning electron microscopy with energy-dispersive X-ray spectroscopy (SEM-EDS). Minerals were crushed with a tungsten carbide mill (94% tungsten carbide and 6% cobalt, Retsch model RS100) and sieved to a maximum diameter of 106 µm with a Retsch AS 200 sieve. The resulting particle size distribution ranged from 1 to 160 µm with an average diameter of 40 μm for Mag and from 0.1 to 400 μm (due to the formation of particle aggregates) with an average diameter of 111 µm for Py. Particle size distribution of the cast Fe(0) (92% purity, Gotthart Maier Metallpulver GmbH) ranged from 0.4 to 2.0 mm, with an average diameter of 1.2 mm. According to the provider the particle size distribution for nano-sized Fe(0) (99%, Sigma-Aldrich) ranged from 40 to 60 nm. The milli-sized Fe(0), nano-sized Fe(0) and micro-sized Fe-bearing minerals were acid-cleaned to increase surface area, dissolve any unreactive oxide or organic coating (Matheson and Tratnyek, 1994; Slater et al., 2002) and obtain a reproducible surface (Kriegman-King and Reinhard, 1994). Milli-sized Fe(0) and minerals were soaked in degassed 0.1 M hydrochloric solution (HCl, 32 wt %, Sigma-Aldrich) for 1 h, while for nano-sized Fe(0), soaking was done for 5 min. All the solids were rinsed five times with degassed deionized water and dried overnight (Matheson and Tratnyek, 1994; Slater et al., 2002). Py and Mag samples were dried in an oven (Technopyro model PR4T) at 100 °C in closed serum bottles and lyophilized afterwards (Telstar Cryodos-45 2001 n°376) to remove remaining water. Specific surface area was measured by BET for milli-sized Fe(0), Py and Mag before $(1.00\pm0.01, 0.830\pm0.005, 0.62\pm0.01 \text{ m}^2/\text{g}, \text{respectively})$ and after acid cleaning $(1.624\pm0.007, 2.47\pm0.02, 0.698\pm0.003 \text{ m}^2/\text{g}, \text{respectively})$. For nano-sized Fe(0), it was only measured before cleaning $(11.16\pm0.09 \text{ m}^2/\text{g})$.

3. Sampling and preservation

Except for the nano-sized Fe(0) experiments, reactions were stopped by filtration with 0.2 μm-filters Mille-LG PTFE LCR (Merck Millipore) at different time intervals. Small aliquots were taken for pH measurements before filtration. At pH 12, the filtered solution was neutralized by acetic acid for quenching the alkaline hydrolysis reaction. Samples were held at 4 °C until analysis in 12-mL glass vials covered with aluminum foil (Elsner et al., 2006) for the milli-sized Fe(0) experiments; and in 12-mL vials amber glass vials for the Mag and Py experiments. In the case of the nano-sized Fe(0) experiments, 0.1 mL of headspace were taken from each single 42-mL vial for measuring CT and CF concentrations and carbon and chlorine isotope analyses by direct injection in the equipment. For concentration estimation, calculations of total mM in the liquid phase considering Henry's law constant at 24 °C (Staudinger and Roberts, 2001) were performed.

4. Analytical methods

pH measurements

pH evolution was monitored using a Crison pH2001 n°6037 (Crison, Spain) in the experiments with Py and Mag and by using a Labor-pH-Meter Lab 850 Messparameter (SI-Analytics, Germany) in the Fe experiments.

BET

Specific surface areas were determined by the BET (Brunauer–Emmett–Teller) gas adsorption method with a TriStar 3000 V6.04 micromeritics surface area analyzer using 5-point N₂ adsorption isotherms (Brunauer et al., 1938) in *Centres científics i tecnològics de la Universitat de Barcelona* (CCiT-UB).

Particle size distribution

Milli-sized iron, Py and Mag particle size distribution was determined using a particle size analyzer by photon correlation spectroscopy (Beckman Coulter, model N5) between 0.04 to 2000 µm in *Laboratori de Sedimentologia* (UB).

SEM-EDS

Unaltered and crushed Py and Mag were studied with a scanning electron microscope Quanta 200 FEI XTE 325/D8395 coupled with Energy-dispersive X-ray spectroscopy Genesi (EDAX) in CCiT-UB.

X-ray analyses

X-ray powder diffraction measurements were performed in CCiT-UB on homogenized sample aliquots using a Bragg–Brentano $\theta/2\theta$ PANalytical X'Pert PRO MPD Alpha1 powder diffractometer (radius = 240 mm) with Cu K α_1 radiation, selected by means of a Focalizing Ge (111) primary monochromator. Experimental conditions: sample spinning at 2 revolutions per second; variable automatic divergence slit to get an illuminated length in the beam direction of 10 millimetres; mask defining a length of the beam over the sample in the axial direction of 12 millimetres; diffracted beam of 0.04 radians *Soller* slits; X'Celerator Detector with Active length of 2.122 °. The starting and the final 2 θ angles were 4° and 80°, respectively. The step size was 0.017° 2 θ and the measuring time, 150 s per step. Mineral identification was made using the X'Pert HighScore software (Degen et al., 2014).

5. Experimental conditions

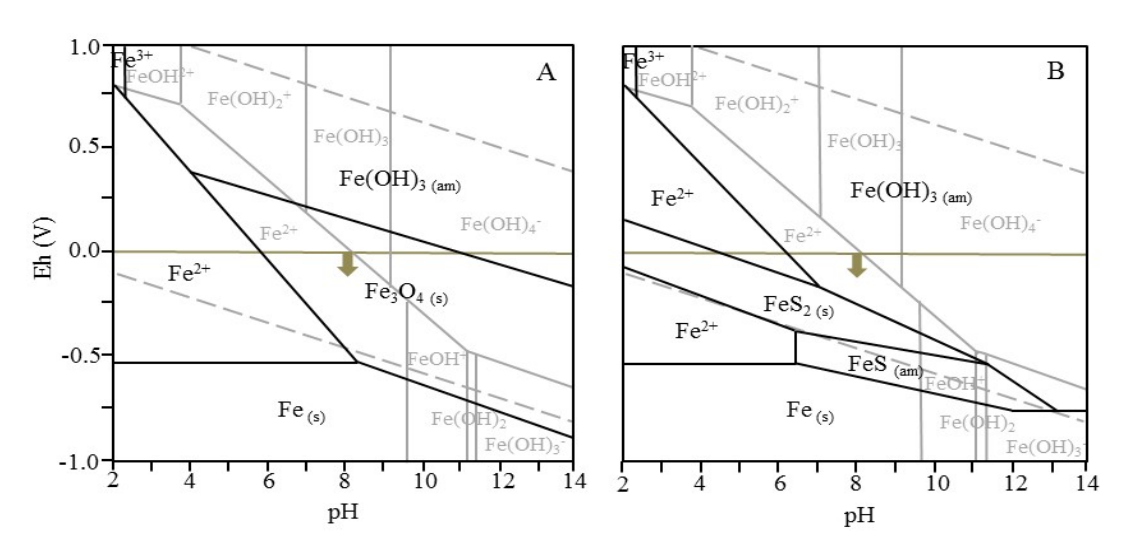
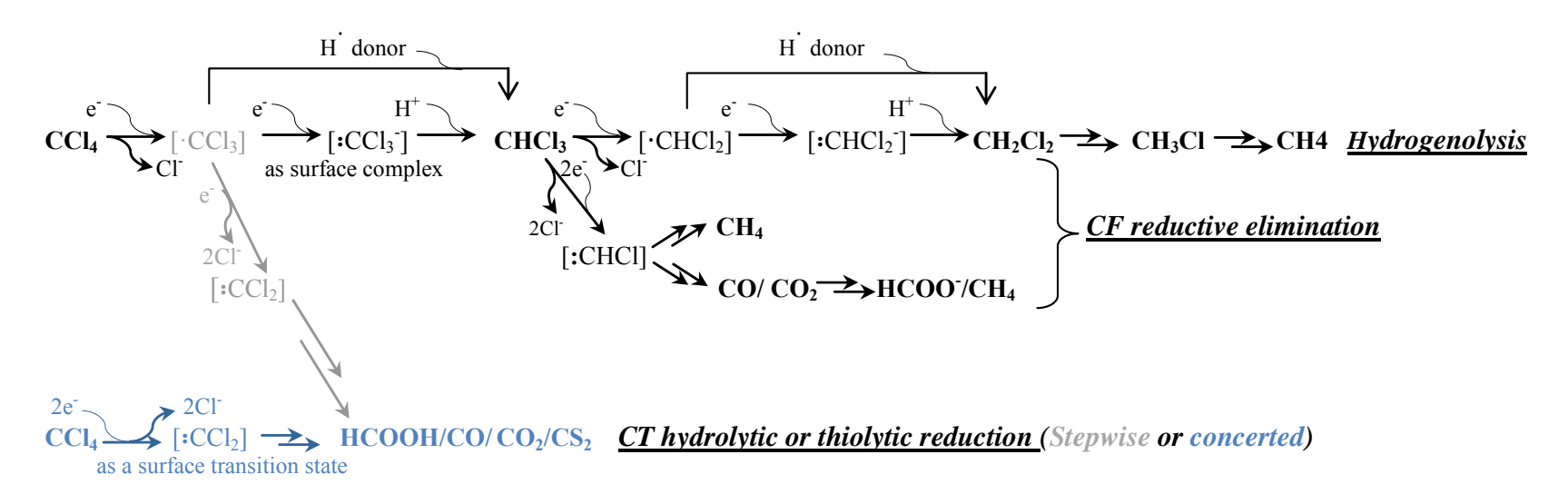


Fig. S1. Eh-pH predominance diagrams of Fe-Cl-H₂O (A) and Fe-Cl-S-H₂O (B) systems. Fe₃O₄ (Mag) is not allowed to form in B. Calculations were performed using the code MEDUSA (Puigdomènech, 2010) and with $[Cl^-]_{tot}$: 1.2 mM, $[Fe^{2+}]_{tot}$: 0.6 mM and $[SO_4^{2-}]_{tot}$: 10 μ M. In grey, aqueous species are represented. The arrow indicates assumed Eh experimental conditions and the dashed lines, water stability field.

6. Degradation pathways



Scheme S1. Discussed CT and CF abiotic reductive degradation pathways. The double arrow indicates omitted intermediate steps for simplification

7. pH evolution

In the CT experiments at pH 7, acidic conditions occurred during the first days, especially in the case of the CT_Py_7 experiment, for which pH remained acidic during all the experimental period (4.7±1.1) (Fig. S2). In the presence of Py at pH 12, however, the pH was kept constant (11.8±0.2) during the course of the experiment (Fig. S2). This different behavior between pH values in homologous experiments is consistent with previous studies, which concluded that in all Py oxidizing systems, pH tends to reach more acidic values but when pH is higher than 11, the pH decrease is much slower than at neutral pH values (Bonnissel-Gissinger et al., 1998). However, this pH decrease was not observed in CF_Py_7 experiment, which suggested low Py oxidizing capacity towards CF.

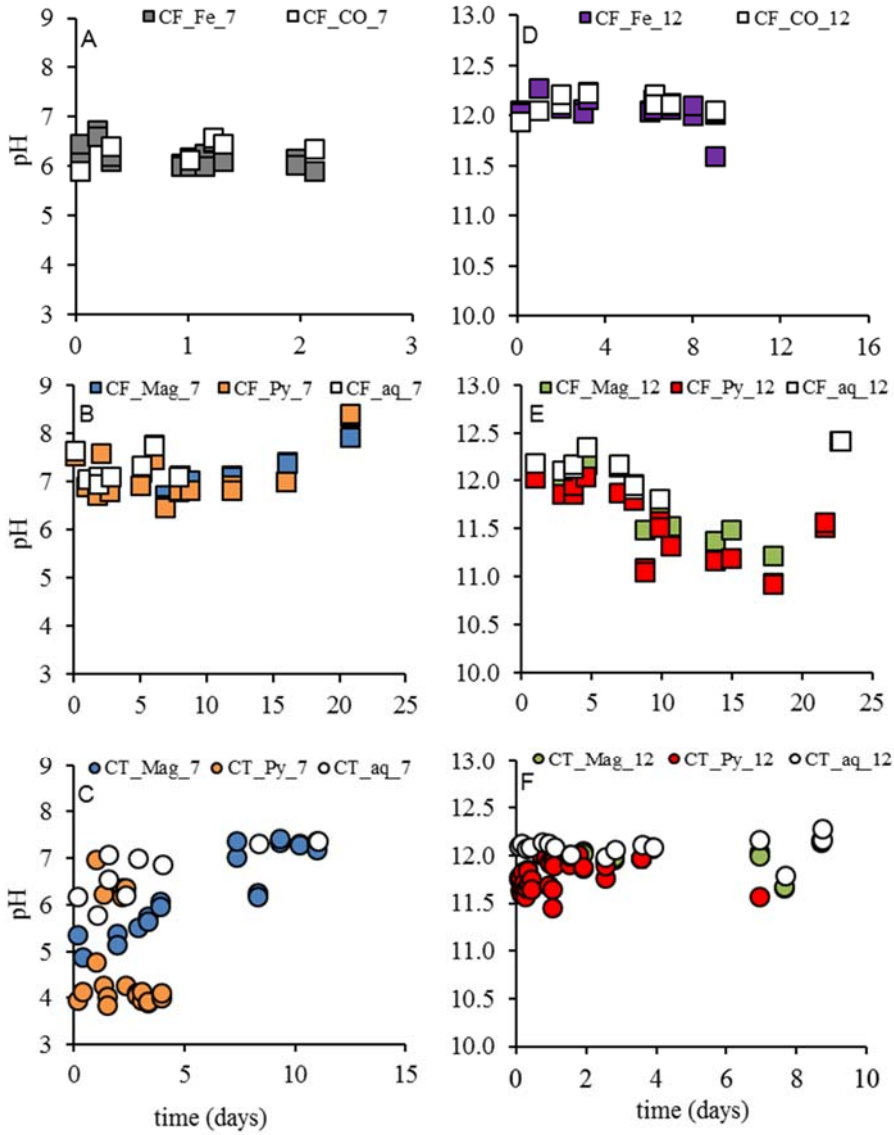


Fig. S2. pH evolution over time in the pH 7 experiments (left): CF_Fe_7 and CF_CO_7 (A, from Torrentó et al., 2017); CF_Mag_7, CF_Py_7 and CF_aq_7 (B); CT_Mag_7, CT_Py_7 and CT_aq_7 (C); and in the pH 12 experiments (right): CF_Fe_12 and CF_CO_12 (D); CF_Mag_12, CF_Py_12 and CF_aq_12 (E) CT_Mag_12, CT_Py_12 and CT_aq_12 (F). Error bars are smaller than the symbols.

8. Degradation study by Fe(0)

Kinetics of Fe(0) experiments

Assuming that all the removal of CT or CF is due to a degradation process, data for CT and CF aqueous concentration versus time can be fitted to a pseudo-first-order rate model following Eq. S1, in order to compare kinetics among pH 7 and pH 12 and to those from the literature (Table S1, S3).

$$dC/dt = -k'C$$
 (S1)

C is the target chlorinated compound concentration in μ mol/L, t is time in hours and k' is the pseudo-first-order rate constant (h⁻¹). The k' was obtained using the integrated form of Eq. S1, as shown in Eq. S2, where C_{θ} is the initial concentration of the chlorinated compound (μ mol/L). Uncertainty was obtained from 95% confidence intervals (CI).

$$lnf=lnC/C_0=k't$$
 (S2)

When possible, a surface-area-normalized reaction rate constant (k_{SA} , L m⁻² h⁻¹) was calculated for comparison with other studies (Table S1, S3) as described by Eq. S3 (Matheson and Tratnyek, 1994; Johnson et al., 1996):

$$dC/dt = -k'C = -k_{SA} a_S \rho_m C$$
 (S3)

where a_S is the specific surface area of metal and ρ_m is the mass concentration of Fe(0).

The k_{SA} values for CT_Fe_7 and CT_Fe_12 experiments are within the range of some values reported in literature (Table S1) for CT degradation by Fe(0) or by FeS, but there are discrepancies with other types of Fe(0) or Fe-bearing minerals (He et al., 2015). Similarly, the k_{SA} values for CF_Fe_7 and CF_Fe_12 experiments are lower than for nano-sized experiments (Table S1). This confirms, as stated by Johnson et al. (1996), that variability in pollutant disappearance rates despite surface area normalization is high, being attributable to different Fe(0) pre-treatment, 'non-reactive' sites amount and experimental conditions (Noubactep, 2009).

Table S1. Degradation products, pseudo first-order rate constants (k) and surface area normalized rate constants (k_{SA}) of abiotic degradation of chlorinated methanes by Fe(0) under anoxic conditions. n.m. =not measured.

Pollutant	Fe(0)	Conditions	Degradation product	k'(h-1)	k _{SA} (Lm ⁻² ·h ⁻¹)	Reference			
CT	Nano: 11.2 m ² /g	pH 7	CF	1.4 ± 0.2 $R^2 = 0.95$	(4.9±0.6)×10 ⁻²	This study			
CI	40-60 nm	pH 12	CF	1.24 ± 0.04 $R^2 = 0.99$	(4.4±0.1)×10 ⁻²	This study			
CT	Nano 27.9 m²/g	Buffered pH 7.5 Unbuffered Unbuffered	CF, DCM, CH ₄	5.0±0.4 2.2±0.1 2.2±0.1	1.1±0.1 0.48±0.04 0.49±0.04	Song and Carraway (2006)			
CT	$2.4 \text{ m}^2/\text{g} \sim 10 \mu\text{m}$	pH 7.7, 1g Fe(0) pH 7.7, 10g Fe(0)	CF, DCM	0.30-0.45 1.72-2.21	2.8-4.1×10 ⁻² 1.9-2.5×10 ⁻²	Helland et al. (1995)			
CT	0.09±0.03 m ² /g 0.20±0.02 m ² /g, 7.4±0.2 m ² /g 1.79±0.07 m ² /g	pH 7 pH 7 pH 7 pH 7 pH 12	CF	0.47±0.06 0.6±0.1 0.12±0.04 0.4±0.1 0.04±0.01	$(4.2\pm0.5)\times10^{-4}$ $(2.3\pm0.4)\times10^{-3}$ $(4.0\pm1.4)\times10^{-3}$ $(2.6\pm0.9)\times10^{-2}$ $(1.6\pm0.4)\times10^{-4}$	Támara and Butler (2004)			
CT	<100 nm	- pii 12	CF, DCM,CH ₄	0.5-2.2	5.4×10 ⁻⁴ -1.01	Lien and Zhang (1999)			
СТ	Micro: 0.22 m ² /g	EDTA (organic ligand) pH 3.5-7.5	CF, DCM	0.843-0.280	(6.5-2.1)×10 ⁻³	Zhang et al. (2011)			
		pH 3.5-7.5		0.021-0.005	(1.7-0.4)×10 ⁻⁴				
		Ultrapure water		6±1	9.60±1.92×10 ⁻²				
	Nano 26 m²/g 100 nm	Humic acid (50-1000 mg/L)		5-3	6.92-4.12×10 ⁻²				
CT		Surfactant SDS (1-2.4mM)	Not studied	1-2	1.82-2.46×10 ⁻²	Feng et al. (2008)			
		Surfactant CTAB (0.1-10mM)		10-9	14.7-14.5×10 ⁻²				
		Surfactant NPE (0.02-1mM)		5-7	7.95-10.9×10 ⁻²				
CF	Milli 77 m ² /L (1.00 ± 0.01) m ² /g	pH 12.1±0.1	DCM	$(4.6\pm1.9)\times10^{-3}$ $R^2 = 0.67$	(5.9±2.5)×10 ⁻⁵	This study			
CF	Milli $(1.00\pm0.01) \text{ m}^2/\text{g}$	pH 6.3±0.2	DCM	$(7\pm1)\times10^{-2}$ $R^2 = 0.93$	(9±2)×10 ⁻⁴	Torrentó et al. (2017)			
		Ultrapure water		(1.3±0.3)×10 ⁻²	1.9±0.5×10 ⁻⁴				
		Humic acid (50-1000 mg/L)		2-32×10 ⁻²	3-50×10 ⁻⁴				
CF	Nano 26 m²/g 100 nm	Surf. SDS (1-2.4mM)	Not studied	2-8×10 ⁻²	3-13×10 ⁻⁴	Feng et al. (2008)			
		Surf. CTAB (0.1-10mM)		2-4×10 ⁻²	2-5×10 ⁻⁴				
		Surf. NPE (0.02-1mM)		2-1×10 ⁻²	2-5×10 ⁻⁴				
		Buffered pH 7.5		1.9±0.2	4.2±0.5				
CF	Nano	unbuffered	DCM, CH ₄	1.4±0.1	3.1±0.3	Song and Carraway (2006)			
Cr	27.9 m ² /g	Equilibrated (unbuffered)	DC171, C114	1.5±0.1	3.3±0.3	Song and Carraway (2000)			

<u>Isotopic fractionation of Fe(0) experiments</u>

The extent of a contaminant transformation for a defined reaction in terms on stable isotope ratios can be determined by its isotopic fractionation (ϵ) following the Rayleigh approach (Eq. S4), where δ_0 and δ_t are isotope values in the beginning (0) and at a given time (t), respectively, and f is the fraction of substrate remaining at time t.

Isotope signatures are usually reported in per mil (‰) using the delta notation relative to international standards, i.e. Vienna PeeDee Belemnite for carbon ($\delta^{13}C_{VPDB}$) and the international Standard Mean Ocean Chloride (SMOC) for chlorine ($\delta^{37}Cl_{SMOC}$).

$$\ln\left(\frac{\delta_t + 1}{\delta_0 + 1}\right) = \varepsilon \times \ln f \tag{S4}$$

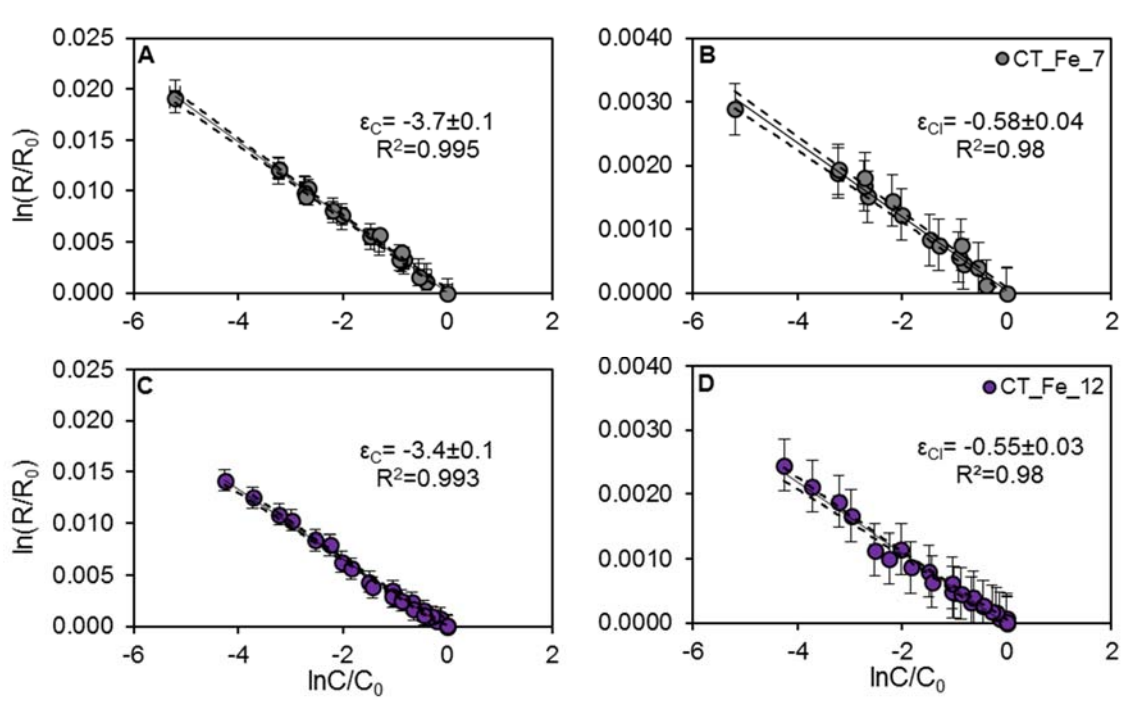


Fig. S3. Logarithmic plots according to Rayleigh equation (Eq. S4) of carbon (A, C panels) and chlorine (B, D panels) isotope ratios during CT reductive dechlorination by Fe(0) at pH 7 (upper panels) and at pH 12 (lower panels). ϵ C and ϵ Cl values are given. Dashed lines represent 95% CI of the linear regression. Error bars display the uncertainty calculated by error propagation including uncertainties in concentration (5%) and isotope measurements (0.5% for ϵ 13C and 0.2% for ϵ 37Cl). In some cases, error bars are smaller than the symbols.

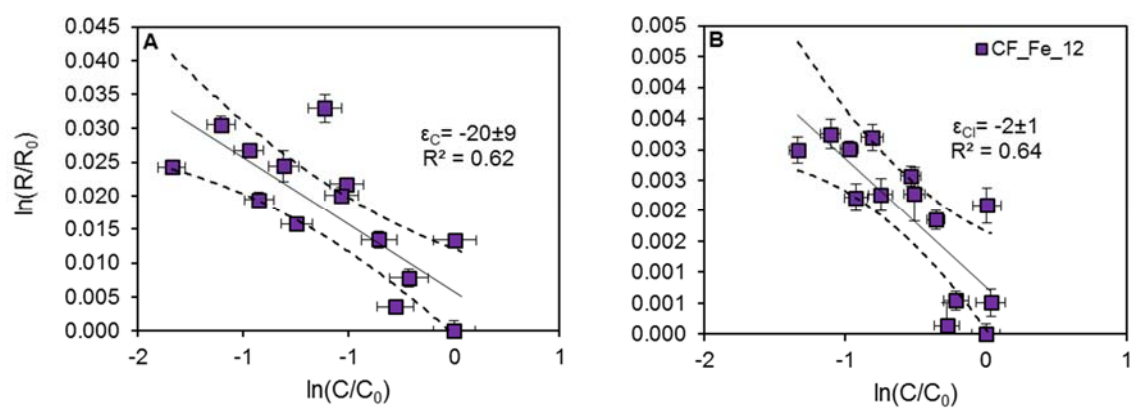


Fig. S4. Logarithmic plots according to Rayleigh equation (Eq. S4) of carbon (A) and chlorine (B) isotope ratios during CF reductive dechlorination by Fe(0) at pH 12. EC and ECl values are given. Dashed lines represent 95% CI of the linear regression. Error bars display the uncertainty calculated by error propagation including uncertainties in concentration (5%) and standard deviation of duplicates in isotope measurements. In some cases, error bars are smaller than the symbols.

Calculation of Apparent Kinetic Isotope Effects (AKIE)

Carbon and chlorine AKIE values were calculated following Eq. S5 (Elsner et al., 2005), where n is the number of atoms of the considered element in the molecule, x is the number of these atoms located at the reactive site/s, and z is the number of atoms located at the reactive site/s and being in intramolecular competition. AKIE_C of CT in the CT_Fe_7 and CT_Fe_12 experiments was calculated using n=x=z=1, while for AKIE_{Cl}, n=x=z=4 was used. The uncertainty of the AKIE was estimated by error propagation in Eq. S7. The results of these experiments were compared to reductive dechlorination studies reported in literature in Table S2.

$$AKIE_{E} \approx \frac{1}{1 + \left(\frac{z \times n}{x} \times \frac{\varepsilon}{1000}\right)}$$
 (S5)

Carbon isotopic mass balance

Carbon isotopic mass balance ($\delta^{13}C_{SUM}$) was calculated following Eq. (S6) (Hunkeler et al., 1999; Aeppli et al., 2010) where x is the molar fraction of each compound relative to the total molar CMs mass from those isotopic values that are available in each experiment. The uncertainty of $\delta^{13}C_{SUM}$ was determined by error propagation in Eq. S6.

$$\delta^{13}C_{SUM} (\%) = x_{CT}\delta^{13}C_{CT} + x_{CF}\delta^{13}C_{CF} + x_{DCM}\delta^{13}C_{DCM}$$
 (S6)

The extent of degradation and pathway-specific contributions

Assuming that only one degradation process occurs, the extent of degradation (D) can be estimated using the expression derived from the Rayleigh equation (Eq. S7), where δ_0 and δ_t are isotope values in the beginning (0) and at a given time (t), respectively and ϵ is the isotope fractionation of the transformation reaction under consideration.

$$D(\%) = \left[1 - \left(\frac{\delta_t + 1000}{\delta_0 + 1000}\right)^{\frac{1000}{\varepsilon}}\right] \times 100$$
(S7)

Pathway-specific contributions to total degradation of a pollutant may be estimated using the expression derived by Van Breukelen (2007) (Eq. S8), where F is the distribution of pathways 1 and 2; ε C and ε Cl are the C and Cl isotope fractionation values of the two pathways, respectively and Λ is the obtained dual C-Cl isotope slope for a target pollutant.

$$F = \frac{\Lambda \mathcal{E}_1^{Cl} - \mathcal{E}_1^{C}}{\left(\mathcal{E}_2^{C} - \mathcal{E}_1^{Cl}\right) - \Lambda \left(\mathcal{E}_2^{Cl} - \mathcal{E}_1^{Cl}\right)}$$
(S8)

Summary of \mathcal{E} , AKIE and Λ values from studied and reported experiments

Table S2. Comparison of ϵ and AKIE values for C and Cl isotopes in different reductive dechlorination studies. n.m.: not measured; n.ap.: not available;

Compound	Degradation pathway	Туре	Conditions	ε _{bulkC} (‰) ± 95%CI	n _C	ХC	ZC	AKIE _C	ε _{bulkCl} (‰) ± 95%CI	n _{Cl}	XCI	ZCI	AKIEcı	Λ≈εC/εCl	Reference
Reductive dechlorination by C-Cl bond cleavage		Streitwieser limit KIE _C = 1.057 (Elsner et al., 2005; Aelion et al., 2010) Streitwieser limit KIE _C = 1.013 (Elsner et al., 2005)										al., 2005)			
CF	Reductive dechlorination	abiotic Fe(0) pH 7	laboratory	-33 ± 11	1	1	1	1.034 ± 0.012	-3 ± 1	3	3	3	1.008 ± 0.001	8 ± 2	Torrentó et al. (2017)
CF	Reductive dechlorination	abiotic Fe(0) pH 12	laboratory	-20 ± 9	1	1	1	1.020 ± 0.009	-2 ± 1	3	3	3	1.006±0.001	8 ± 1	This study
CF	Reductive dechlorination	abiotic Fe(0)	laboratory	-29.4 ± 2.1	1	1	1	1.030 ± 0.07	n.m.					n.m.	Lee et al. (2015)
CF	Reductive outer- sphere single electron transfer	CO ₂ radical anions	laboratory	-17.7±0.8					-2.6±0.4					6.7 ± 0.4	Heckel et al. (2017)
CF	Reductive dechlorination	biotic (<i>Dehalobacter</i> sp. CF50 consortium)	laboratory	-27.5 ± 0.9	1	1	1	1.028 ± 0.002	n.m.					n.m.	Chan et al. (2012)
CF	Reductive dechlorination	biotic (<i>Dehalobacter</i> sp.UNSWDHB consortium)	laboratory	-4.3 ± 0.5	1	1	1	1.004	n.m.					n.m.	Lee et al. (2015)
CF	Hydrogenolysis ± reductive elimination	Biotic (field slurry) with vitamin B_{12}	laboratory	-14 ± 4	1	1	1	1.014 ± 0.002	-2.4 ± 0.4	3	3	3	$\begin{array}{c} 1.0072 \pm \\ 0.0004 \end{array}$	7 ± 1	Rodríguez-Fernández et al. (2017)
CT	Reductive dechlorination	abiotic (goethite, magnetite, lepidocrocite, hematite, siderite)	laboratory	-26 to -32	1	1	1	1.027 to 1.033	n.m.					n.m.	Zwank et al., (2005); Elsner et al. (2004)
CT	Reductive dechlorination	abiotic (mackinawite)	laboratory	-10.9 to -15.9	1	1	1	1.011 to 1.016	n.m.					n.m.	Zwank et al. (2005); Neumann et al. (2009)
CT	Reductive dechlorination	abiotic (Zn(0))	laboratory	-10.8 ± 0.7	1	1	1	1.01	n.m.					n.m.	Vanstone et al. (2008)
CT	Hydrogenolysis	Nano-sized Fe(0) at pH 7 and pH 12	laboratory	-3.7 and -3.4	1	1	1	1.0037 and 1.0034	-0.58 and - 0.55	4	4	4	1.00233 and 1.00220	5.8 ± 0.4 and 6.1 ± 0.5	This study
CT	Hydrogenolysis Hydrogenolysis	Aqueous FeCl ₂ at pH 12	laboratory	-3 ± 3	1	1	1	1.003 ± 0.003							This study
CT	and thiolytic reduction	Pyrite at pH 7	laboratory	-5 ± 2	1	1	1	1.005 ± 0.002	-1.5±0.4	4	4	4	1.0060 ± 0.0004	2.9 ± 0.5	This study
CT	Hydrogenolysis and thiolytic reduction	Pyrite pH 12	laboratory	-4 ± 1	1	1	1	1.004 ± 0.001	-0.9 ± 0.4	4	4	4	1.0036 ± 0.0004	3.7 ± 0.9	This study
СТ	Hydrogenolysis and hydrolytic reduction?	Magnetite at pH 12	laboratory	-2 ± 1	1	1	1	1.002 ± 0.001	-0.8±0.2	4	4	4	1.0032±0.000 2	2 ± 1	This study

СТ	Hydrogenolysis among other reductions	Biotic (field slurry)	laboratory	-16 ± 6	1	1	1	1.016 ± 0.001	-6 ± 3	4	4	4	1.023 ± 0.003	6.1 ± 0.5	Rodríguez-Fernández et al. (2017)
СТ	Reduction processes	Biotic (field slurry) with vitamin B ₁₂	laboratory	-13 ± 2	1	1	1	1.013 ± 0.003	-4 ± 2	4	4	4	1.015 ± 0.002	5 ± 1	Rodríguez-Fernández et al. (2017)
1,1,1-TCA	Reductive dechlorination	abiotic (Cr(II), Fe0 and Cu and Fe mixtures)	laboratory	-16 to -14	2	1	1	1.027 ± 0.002	n.m.					n.m.	Elsner et al. (2007)
1,1,1-TCA	Reductive dechlorination	abiotic (Fe(0))	laboratory	-7.8 ± 0.4	2	1	1	1.0158 ± 0.0008	-5.2 ±0.2	3	3	3	1.0160 ± 0.0006	1.5 ± 0.1	Palau et al. (2014)
1,1,1-TCA	Reductive dechlorination	abiotic (hydrolysis/ dehydrohalogenation)	laboratory	-1.6 ± 0.2	2	1	1	1.0033 ± 0.0004	-4.7 ±0.1	3	3	3	1.0145 ± 0.0003	0.33 ± 0.04	Palau et al. (2014)
1,1,1-TCA	Reductive dechlorination	biotic	laboratory	-1.8 to -1.5	2	1	1	1.0036 ±0.0006	n.m.					n.m.	Sherwood Lollar et al. (2010)
1,2-DCA	Reductive dechlorination	abiotic (Zn(0))	laboratory	-29.7 ± 1.5	2	2	1	1.03	n.m.					n.m.	Vanstone et al. (2008)
TCE	Reductive dechlorination	abiotic (Fe(0))	laboratory	-13 ± 2	2	1	1	1.0275	-2.6 ±0.1	3	1	1	1.008 ± 0.001	5.2 ± 0.3	Audí-Miró et al. (2013)
TCE	Reductive dechlorination	abiotic (Fe(0))	field	-12	2	1	1	1.0254	-3.0	3	1	1	1.009	4.2	Lojkasek-Lima et al. (2012)
TCE	Reductive dechlorination	abiotic (FeS)	laboratory	-27.9 to -33.4	2	1	1	1.059 to 1.072	n.m.					n.m.	Liang et al. (2007)
TCE	Reductive dechlorination	abiotic (corrinoids)	laboratory	-15.0 to -18.5					-3.2 to -4.2					0.3 to 0.8	Renpenning et al. (2014)
TCE	Reductive dechlorination	abiotic (vitamin B12)	laboratory	-16.7 to -17.2	2	1	1	1.034 to 1.036	n.m.						Slater et al. (2003)
TCE	Reductive dechlorination	abiotic (cyanocobalamin)	laboratory	-16.1 ±0.9	2	1	1	1.03	-4.0 ±0.2	3	1	1	1.01	3.9 ± 0.2	Cretnik et al. (2013)
TCE	Reductive dechlorination	biotic	laboratory	-8.8 ± 0.2	2	1	1	1.0179	-3.5 ± 0.5	3	1	1	1.0106	2.7 ± 0.1	Wiegert et al. (2013)
TCE	Reductive dechlorination	biotic (KB-1 consortium)	laboratory	-2.5 to -13.8	2	1	1	1.005 to 1.028	n.m.					n.m.	Bloom et al. (2000); Slater et al. (2001)
TCE	Reductive dechlorination	biotic (<i>S. multivorans</i> , <i>D. michiganesis</i> BB1 and BD1 mixed <i>Dehaloc.</i> consortium)	laboratory	-4.1 to -15.3	2	1	1	1.008 to 1.0315	n.m.					n.m.	Liang et al. (2007)
TCE	Reductive dechlorination	biotic (S. multivorans)	laboratory	-20.0 to -20.2					-3.7 to -3.9					5.0 to -5.3	Renpenning et al. (2014)
TCE	Reductive dechlorination	biotic (G. lovleyi SZ, D. hafniense Y51)	laboratory	-9.1 to -12.2	2	1	1	1.02	-2.7 to -3.6	3	1	1	1.01	3.4 ± 0.2	Cretnik et al. (2013)
TCE	Reductive dechlorination	biotic (mixed <i>Dehaloc</i> . consortium)	laboratory	-16.4 ± 0.4	2	2	1	1.017 ± 0.001	-3.6 ± 0.3	3	3	1	1.004 ± 0.000	4.7	Kuder et al. (2013)
PCE	Reductive dechlorination	abiotic (corrinoids)	laboratory	-22.4 to -25.3					-3.4 to - 4.8		_			4.6 to 7.0	Renpenning et al., (2014)
PCE	Reductive dechlorination	abiotic (vitamin B12)	laboratory	-15.8 to -16.5	2	2	2	1.033 to 1.034	n.m.					n.m.	Slater et al. (2003)

PCE	Reductive dechlorination	abiotic (FeS)	laboratory	-24.6 to -30.2	2	2	2	1.052 to 1.064	n.m.					n.m.	Liang et al. (2007)
PCE	Reductive dechlorination	biotic (Desulfitobacterium)	laboratory	-5.6 ± 0.7	2	2	2	1.0113	-2.0 ± 0.5	4	4	4	1.0081	2.5 ± 0.8	Wiegert et al. (2013)
PCE	Reductive dechlorination	biotic (<i>Desulfitobacterium</i> Viet1)	laboratory	-19.0 ±0.9	2	2	2	1.019	-5.0 ±0.1	4	4	4	1.005	3.8 ± 0.2	Cretnik et al. (2014)
PCE	Reductive dechlorination	biotic (Sulfurospirillum, PceATCE)	laboratory	-3.6 ± 0.2	2	2	2	1.007	-1.2 ± 0.1	4	4	4	1.005	2.7 ± 0.3	Badin et al. (2014)
PCE	Reductive dechlorination	biotic (Sulfurospirillum, PceADCE)	laboratory	-0.7 ± 0.1	2	2	2	1.001	-0.9 ±0.1	4	4	4	1.004	0.7 ± 0.2	Badin et al. (2014)
PCE	Reductive dechlorination	biotic (S. multivorans)	laboratory	-1.3 to -1.4					-0.4 to - 0.6					2.2 to 2.8	Renpenning et al.(2014)
PCE	Reductive dechlorination	biotic (<i>S. multivorans</i> , <i>D. michiganesis</i> BB1 and BD1 mixed <i>Dehaloc</i> . consortium)	laboratory	-1.3 to -7.1	2	2	2	1.003 to 1.0415	n.m.					n.m.	Liang et al. (2007)
PCE	Reductive dechlorination	biotic	field	n.ap.				n.ap.	n.ap.				n.ap.	0.42 to 1.12	Wiegert et al. (2012)

9. Degradation study by Fe-minerals and FeCl₂

Kinetics of Mag, Py and aq experiments

Table S3. Degradation products, pseudo first-order rate constants (k_{obs}) and surface area normalized rate constants (k_{SA}) of abiotic degradation of chlorinated methanes by iron minerals under anoxic conditions. n.m.=not measured; n.d.= not detected; n.a.=not available; n.ap.=not aplicable

Pollutant	Mineral phase	Conditions	Degradation product	$k_{obs}(d^{-1})$	k sa (Lm ⁻² d ⁻¹)	Reference	
CT	FeCl ₂ (aq)	pH 12.1±0.1	CF	0.3±0.2	n.ap.	This study	
CT	Magnetite (17 m ² /L)	pH 12.0±0.1	CF	1.4±0.8	(8±5)×10 ⁻² (R ² =0.8)	This study	
CT	Pyrite	pH 4.7 ± 1.1	CF, CS ₂	1.0±0.4	(1.6±0.6)×10 ⁻² (R ² =0.72)	This study	
CT	Pyrite	pH 11.8±0.2	CF, CS ₂	1.2±0.4	(2±1)×10 ⁻² (R ² =0.6)	This study	
CT	Mackinawite (13 m ² /g)	pH 7.2	CF	n.a.	1.2±0.06	(Zwank et al., 2005)	
CT	Mackinawite (77 m ² /g)	pH 7.2	CF	n.a.	(3.0±0.22)×10 ⁻²	(Zwank et al., 2005)	
CT	FeS (33 g/L)	pH 7.5	CF, C ₂ H ₄ , C ₂ H ₆	$(2.98\pm0.22)\times10^{1}$	n.a.	(Choi and Lee, 2009)	
СТ	FeS (200 g/L)	pH 6.5	n.m.	$(4.15\pm0.12)\times10^{1}$	n.a.	(Lipczynska- Kochany et al., 1994)	
СТ	FeS ₂ (200 g/L)	pH 6.5	n.m.	$(4.15\pm0.19)\times10^{1}$	n.a.	(Lipczynska- Kochany et al., 1994)	
CT	FeS fresh (0.73 g/L)	pH 7-8	CF, CS ₂	1.07	n.a.	(Devlin and Muller, 1999)	
CT	FeS aged (0.73 g/L)	pH 7-8	CF, CS ₂	1.24	n.a.	(Devlin and Muller, 1999)	
CT	FeS (18g/L)	-	CF, DCM	9.7×10 ¹	n.a.	(Assaf-Anid and Lin, 2002)	
CT	FeS (0.05 m ² /g). Freeze dried	pH 8.3	CF		5.2±0.62	(Butler and Hayes, 2000)	
СТ	FeS coating on 0.13 g/L Goethite and 0.20 g/L hematite	pH 8.0	CF	0.28±0.14 0.22±0.12	n.a.	(Hanoch et al., 2006)	
CT	Py (0.01 m ² /g; 1.2-1.4 m ² /L)	pH 6.5	CF, CO ₂ , CS ₂ , formate		0.16	(Kriegman-King and Reinhard, 1994)	
CT	Pyrite	Neutral pH	CF	0.22	n.a.	(Devlin and Muller, 1999)	
CT	Pyrrhotite	Neutral pH	CF	0.91	n.a.	(Devlin and Muller, 1999)	
CT	Magnetite	Neutral pH	CF, CH ₄	n.a.	8.9×10 ⁻⁴	(McCormick et al., 2002)	
CT	Green rust	pH 8.0	CF	n.a.	6.23×10 ⁻³	(Liang and Butler, 2010)	
СТ	Green rust (dodecanoate anions)	pH 8±2	CF, HCOOH, CO	1.56 to 2.64	n.a.	(Ayala-Luis et al., 2012)	
CT	Magnetite	pH 7.0	CF, CO	n.a.	4.8×10 ⁻⁴	(Danielsen and Hayes, 2004)	
CT	Magnetite	pH 7.2	CF	n.a.	1.2×10 ⁻¹	(Zwank et al., 2005)	
CT	Magnetite	pH 7.8	CF, CO	n.a.	2.2×10 ⁻² 9.9×10 ⁻⁴	(Vikesland et al., 2007)	
CF	FeCl ₂ (aq)	pH 12.1±0.1	n.d.	(6±3)×10 ⁻² R ² =0.6	n.ap.	This study	
CF	Magnetite	pH 11.8±0.4	n.d.	0.10±0.03 R ² =0.7	(6±2) ×10 ⁻³	This study	
CF	Pyrite	pH 11.5±0.4	DCM	(4±1)×10 ⁻² R ² =0.6	(6±2) ×10 ⁻³	This study	
CF	FeS (0.14 m ² /g)	pH 7.8	n.m.	n.a.	6.1×10 ¹	(Kenneke and Weber, 2003)	

By-products concentration of Mag, Py and aq experiments

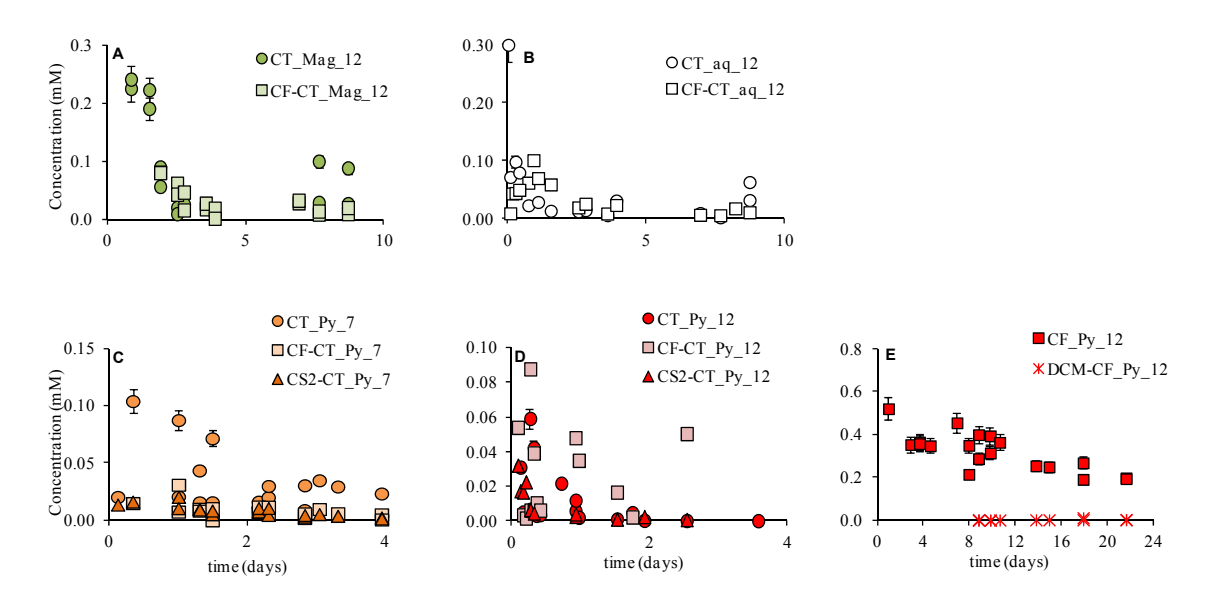


Fig. S5. Concentration (mM) of parent compound (CT or CF) and corresponding by-products (CF, CS_2 or DCM) of those Mag (A), $FeCl_2$ (B) and Py (C,D,E) experiments where by-products were detected.

Isotopic fractionation of Mag, Py and aq experiments

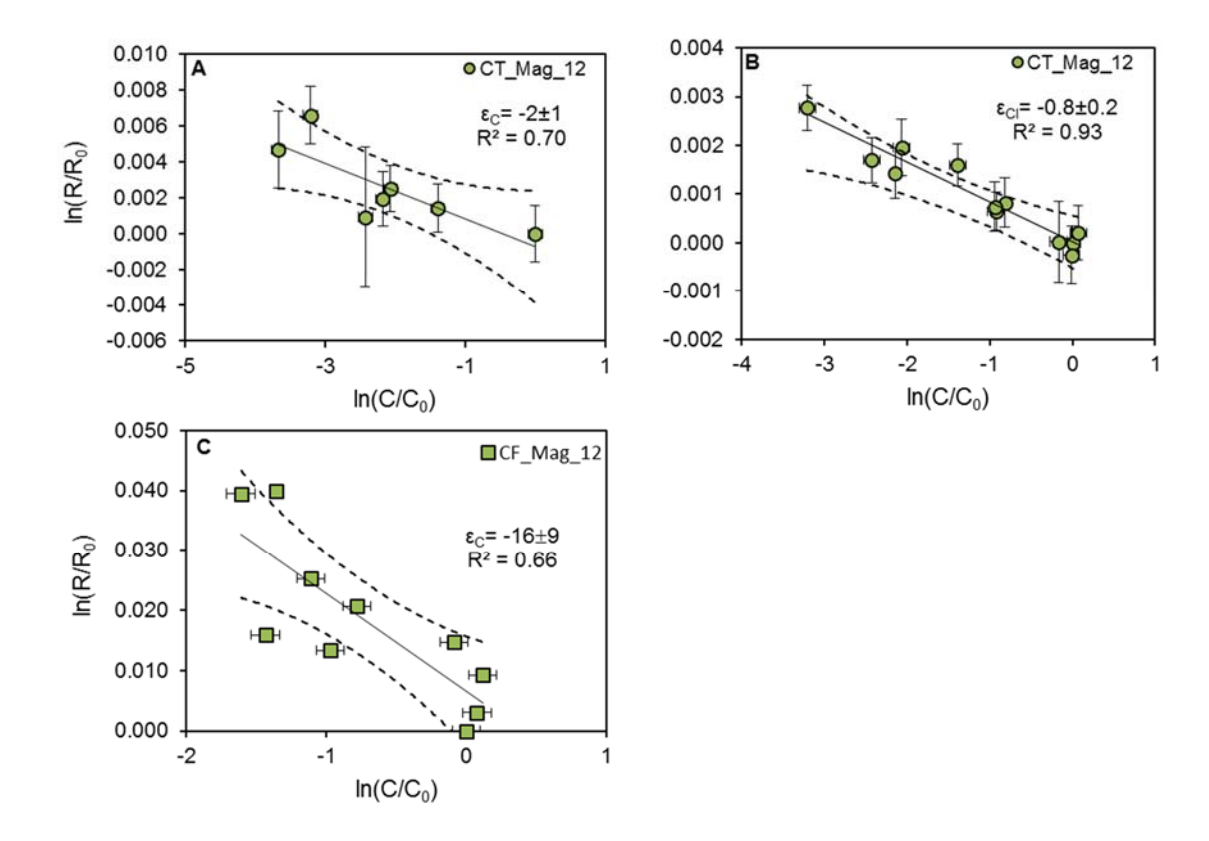


Fig. S6. Logarithmic plots according to Rayleigh equation (Eq. S4) of carbon (A) and chlorine (B) isotope ratios during CT reductive dechlorination by magnetite at pH 12 (upper panels) and carbon isotope ratios during CF reductive dechlorination by magnetite at pH 12 (C). EC and ECl values are given. Dashed lines represent 95% CI of the linear regression. Error bars display the uncertainty calculated by error propagation including uncertainties in concentration (5%) and standard deviation of duplicates in isotope measurements. In some cases, error bars are smaller than the symbols.

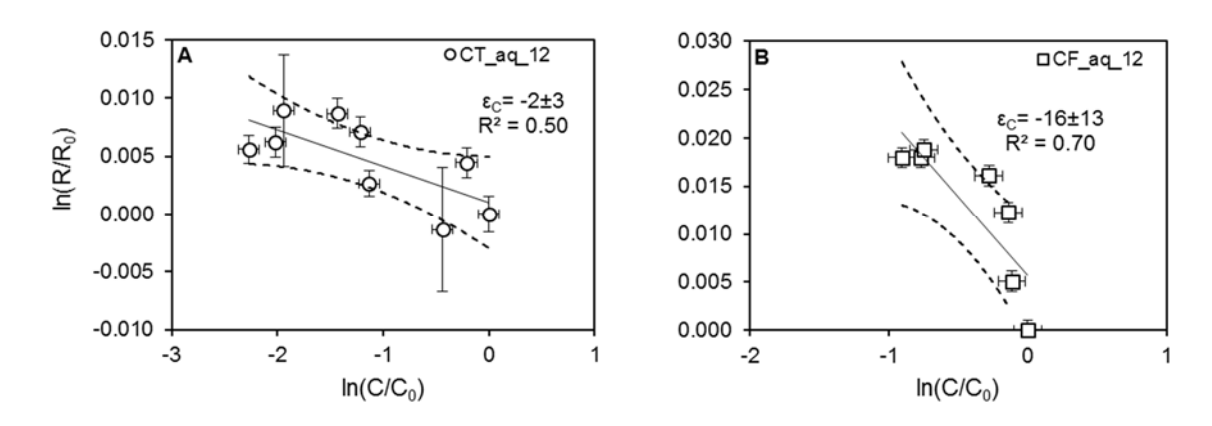


Fig. S7. Logarithmic plots according to Rayleigh equation (Eq. S4) of carbon isotope ratios during CT (A) and CF (B) reductive dechlorination by FeCl₂(aq) at pH 12. EC values are given. Dashed lines represent 95% CI of the linear regression. Error bars display the uncertainty calculated by error propagation including uncertainties in concentration (5%) and standard deviation of duplicates in isotope measurements. In some cases, error bars are smaller than the symbols.

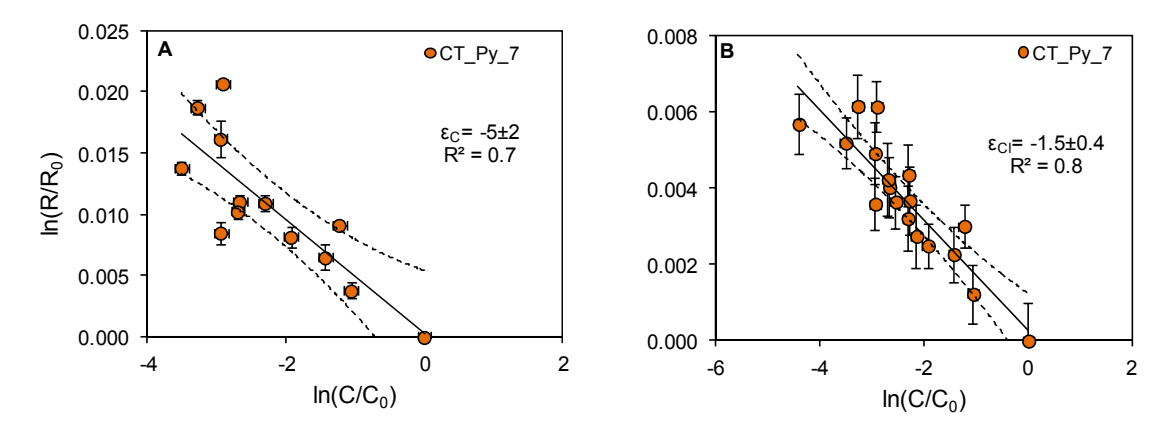


Fig. S8. Logarithmic plots according to Rayleigh equation (Eq. S4) of carbon (A) and chlorine (B) isotope ratios during CT reductive dechlorination by pyrite at pH 7. EC and ECl values are given. Dashed lines represent 95% CI of the linear regression. Error bars display the uncertainty calculated by error propagation including uncertainties in concentration (5%) and standard deviation of duplicates in isotope measurements. In some cases, error bars are smaller than the symbols.

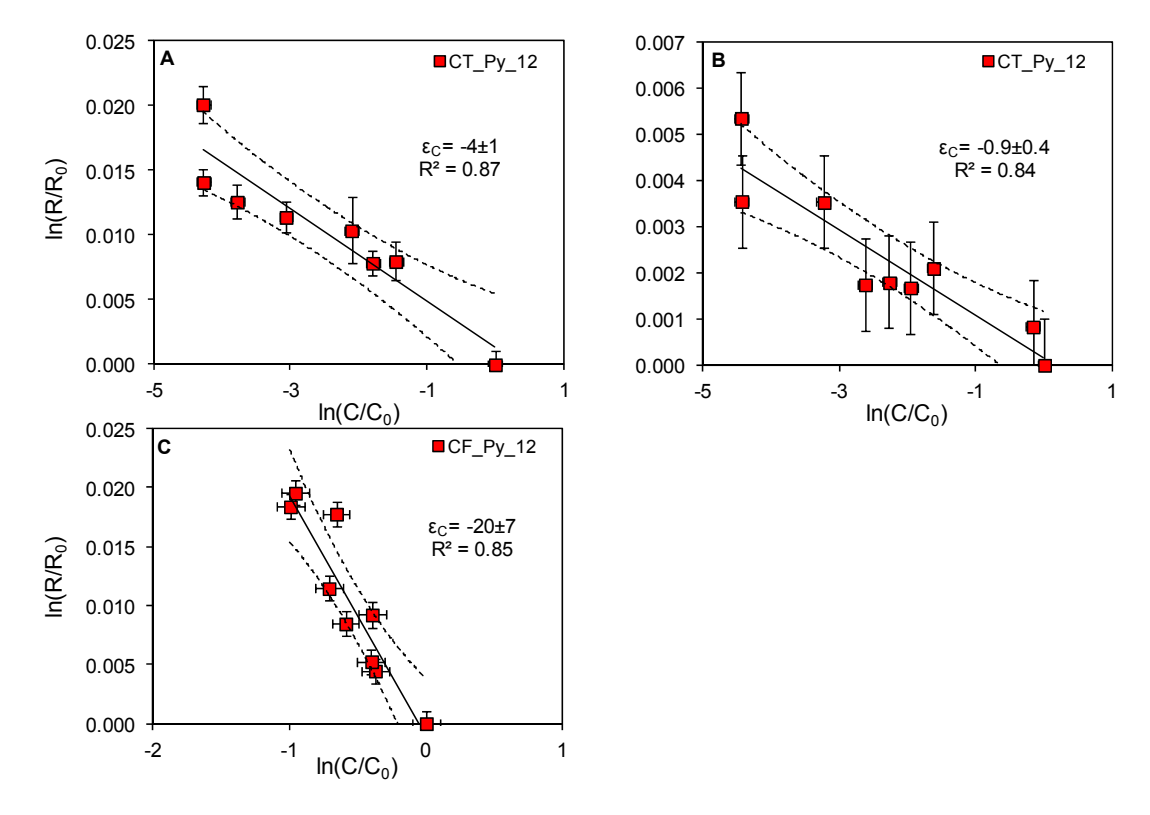


Fig. S9. Logarithmic plots according to Rayleigh equation (Eq. S4) of carbon (A, C) and chlorine (B) isotope ratios during CT (A,B) and CF (B) reductive dechlorination by pyrite at pH 12. EC values are given. Dashed lines represent 95% CI of the linear regression. Error bars display the uncertainty calculated by error propagation including uncertainties in concentration (5%) and standard deviation of duplicates in isotope measurements. In some cases, error bars are smaller than the symbols.

Discussion of CT degradation in Mag experiments at pH 7 and pH 12

Although CT degradation by Mag was not detected in CT_Mag_7 experiments, CT degradation by Mag has been previously reported in the literature. This discrepancy might be attributed to the use in the present experiments of micro-sized Mag in contrast to nano-sized Mag (Hanoch et al., 2006; Maithreepala and Doong, 2007; Vikesland et al., 2007); to the use of a lower Mag/CT ratio than in Zwank et al., (2005); or to the use of different minerals treatments (Hanoch et al., 2006) or different amounts of Fe(II) (Zwank et al., 2005; Vikesland et al., 2007). Total dissolved Fe(II) content was not measured in the present experiments (the theoretical added FeCl₂ amount was 0.6 mM) and thus comparison with previous studies is not straightforward. However, the added 0.6 mM of FeCl₂ was chosen to mimic field conditions since Fe(II) concentrations in anoxic groundwater usually range from 0.009 to 0.179 mM, reaching concentrations up to 0.896 mM (World Health Organization, 2003).

CT degradation with Mag is strongly pH dependent, being faster at higher pH because of the higher density of deprotonated sites at the mineral surface responsible of dechlorination (Danielsen and Hayes, 2004; Lin and Liang, 2013). However, Fe(II) sorption and surface precipitation of Fe(OH)₃(am) onto Mag or other precipitates like green rust are more stable under alkaline conditions and might also contribute on CT degradation (Klausen et al., 1995; Erbs et al., 1999; Liger et al., 1999). In addition, alkaline pH also enhances Fe(II) oxidation to Fe(III) aqueous species (Fig. S1), favoring the CT hydrogenolysis to CF as the overall reaction potential is 0.7 V, while it takes a value below or equal to zero at pH 7. Finally, it is also reported that in nano-sized Mag experiments particle aggregation is expected to decrease as the solution pH increases above or below the pH of isoelectric point (Vikesland et al., 2007), so the available surface to dechlorinate could be higher at pH 12 than at pH 7.

10. References

- Aeppli, C., Hofstetter, T.B., Amaral, H.I.F., Kipfer, R., Schwarzenbach, R.P., Berg, M., 2010. Quantifying in situ transformation rates of chlorinated ethenes by combining compound-specific stable isotope analysis, groundwater dating, and carbon isotope mass balances. Environ. Sci. Technol. 44, 3705–3711. doi:10.1021/es903895b
- Assaf-Anid, N., Lin, K.-Y., 2002. Carbon tetrachloride reduction by Fe²⁺, S²⁻, and FeS with vitamin B_{12} as organic amendment. J. Environ. Eng. 128, 94–99. doi:10.1061/(ASCE)0733-9372(2002)128:1(94)
- Audí-Miró, C., Cretnik, S., Otero, N., Palau, J., Shouakar-Stash, O., Soler, A., Elsner, M., 2013. Cl and C isotope analysis to assess the effectiveness of chlorinated ethene degradation by zero-valent iron: Evidence from dual element and product isotope values. Appl. Geochemistry 32, 175–183. doi:10.1016/j.apgeochem.2012.08.025
- Ayala-Luis, K.B., Cooper, N.G.A., Koch, C.B., Hansen, H.C.B., 2012. Efficient dechlorination of carbon tetrachloride by hydrophobic green rust intercalated with dodecanoate anions. Environ. Sci. Technol. 46, 3390–3397. doi:10.1021/es204368u
- Badin, A., Buttet, G., Maillard, J., Holliger, C., Hunkeler, D., 2014. Multiple dual C-Cl isotope patterns associated with reductive dechlorination of tetrachloroethene. Environ. Sci. Technol. 48, 9179–9186. doi:10.1021/es500822d
- Bloom, Y., Aravena, R., Hunkeler, D., Edwards, E., Frape, S.K., 2000. Carbon isotope fractionation during microbial dechlorination of trichloroethene, cis-1,2-dichloroethene, and vinyl chloride: implications for assessment of natural attenuation. Environ. Sci. Technol. 34, 2768–2772. doi:10.1021/es991179k
- Bonnissel-Gissinger, P., Alnot, M., Ehrhardt, J.J., Behra, P., 1998. Surface oxidation of pyrite as a function of pH. Environ. Sci. Technol. 32, 2839–2845. doi:10.1021/es980213c
- Brunauer, S., Emmett, P.H., Teller, E., 1938. Adsorption of gases in multimolecular layers. J. Am. Chem. Soc. 60, 309–319. doi:citeulike-article-id:4074706
- Butler, E.C., Hayes, K.F., 2000. Kinetics of the transformation of halogenated aliphatic compounds by iron sulfide. Environ. Sci. Technol. 34, 422–429. doi:10.1021/es980946x
- Chan, C.C.H., Mundle, S.O.C., Eckert, T., Liang, X., Tang, S., Lacrampe-Couloume, G., Edwards, E.A., Sherwood Lollar, B., 2012. Large carbon isotope fractionation during biodegradation of chloroform by *Dehalobacter* cultures. Environ. Sci. Technol. 46, 10154– 10160. doi:10.1021/es3010317
- Choi, K., Lee, W., 2009. Reductive dechlorination of carbon tetrachloride in acidic soil manipulated with iron(II) and bisulfide ion. J. Hazard. Mater. 172, 623–630. doi:10.1016/j.jhazmat.2009.07.041
- Cretnik, S., Bernstein, A., Shouakar-Stash, O., Löffler, F., Elsner, M., 2014. Chlorine isotope effects from isotope ratio mass spectrometry suggest intramolecular C-Cl bond competition in trichloroethene (TCE) reductive dehalogenation. Molecules 19, 6450–6473. doi:10.3390/molecules19056450
- Cretnik, S., Thoreson, K.A., Bernstein, A., Ebert, K., Buchner, D., Laskov, C., Haderlein, S., Shouakar-Stash, O., Kliegman, S., McNeill, K., Elsner, M., 2013. Reductive dechlorination of TCE by chemical model systems in comparison to dehalogenating bacteria: Insights from dual element isotope analysis (\begin{subarray}{c} \begin{subarray}{c} \alpha \end{subarray} \begin{subarray}{c} \alpha \end{subarray}

- Danielsen, K.M., Hayes, K.F., 2004. pH dependence of carbon tetrachloride reductive dechlorination by magnetite. Environ. Sci. Technol. 38, 4745–4752. doi:10.1021/es0496874
- Degen, T., Sadki, M., Bron, E., König, U., Nénert, G., 2014. The HighScore suite. Powder Diffr. 29, S13–S18. doi:10.1017/S0885715614000840
- Devlin, J.F., Muller, D., 1999. Field and laboratory studies of carbon tetrachloride transformation in a sandy aquifer under sulfate reducing conditions. Environ. Sci. Technol. 33, 1021–1027. doi:10.1021/es9806884
- Elsner, M., Cwiertny, D.M., Roberts, A.L., Sherwood Lollar, B., 2007. 1,1,2,2-Tetrachloroethane reactions with OH⁻, Cr(II), granular iron, and a copper iron bimetal: insights from product formation and associated carbon isotope fractionation. Environ. Sci. Technol. 41, 4111–4117. doi:10.1021/es072046z
- Elsner, M., Haderlein, S.B., Kellerhals, T., Luzi, S., Zwank, L., Angst, W., Schwarzenbach, R.P., 2004. Mechanisms and products of surface-mediated reductive dehalogenation of carbon tetrachloride by Fe(II) on goethite. Environ. Sci. Technol. 38, 2058–2066. doi:10.1021/es034741m
- Elsner, M., Lacrampe-Couloume, G., Sherwood Lollar, B., 2006. Freezing to preserve groundwater samples and improve headspace quantification limits of water-soluble organic contaminants for carbon isotope analysis. Anal. Chem. 78, 7528–7534. doi:10.1021/ac061078m
- Elsner, M., Zwank, L., Hunkeler, D., Schwarzenbach, R.P., 2005. A new concept linking observable stable isotope fractionation to transformation pathways of organic pollutants. Environ. Sci. Technol. 39, 6896–6916. doi:10.1021/es0504587
- Erbs, M., Christian, H., Hansen, B., Olsen, C.E., 1999. Reductive dechlorination of carbon tetrachloride using iron (II) iron (III) hydroxide sulfate (green rust). Environ. Sci. Technol. 33, 307–311. doi:doi:10.1021/es980221t
- Feng, J., Zhu, B. wei, Lim, T.T., 2008. Reduction of chlorinated methanes with nano-scale Fe particles: Effects of amphiphiles on the dechlorination reaction and two-parameter regression for kinetic prediction. Chemosphere 73, 1817–1823. doi:10.1016/j.chemosphere.2008.08.014
- Hanoch, R.J., Shao, H., Butler, E.C., 2006. Transformation of carbon tetrachloride by bisulfide treated goethite, hematite, magnetite, and kaolinite. Chemosphere 63, 323–334. doi:10.1016/j.chemosphere.2005.07.016
- He, Y.T., Wilson, J.T., Su, C., Wilkin, R.T., 2015. Review of abiotic degradation of chlorinated solvents by reactive iron minerals in aquifers. Groundw. Monit. Remediat. 35, 57–75. doi:10.1111/gwmr.12111
- Heckel, B., Cretnik, S., Kliegman, S., Shouakar-Stash, O., McNeill, K., Elsner, M., 2017. Reductive outer-sphere single electron transfer is an exception rather than the rule in natural and engineered chlorinated ethene dehalogenation. Environ. Sci. Technol. 51, 9663–9673. doi:10.1021/acs.est.7b01447
- Helland, B.R., Alvarez, P.J.J., Schnoor, J.L., 1995. Reductive dechlorination of carbon tetrachloride with elemental iron. J. Hazard. Mater. 41, 205–216. doi:10.1016/0304-3894(94)00111-S
- Hunkeler, D., Aravena, R., Butler, B.J., 1999. Monitoring microbial dechlorination of tetrachloroethene (PCE) using compound-specific carbon isotope ratios: Microcosms and

- field experiments. Environ. Sci. Technol. 33, 2733-2738. doi:10.1021/es981282u
- Johnson, T.L., Scherer, M.M., Tratnyek, P.G., 1996. Kinetics of halogenated organic compound degradation by iron metal. Environ. Sci. &Technology 30, 2634–2640. doi:S0013-936X(96)00090-9
- Kenneke, J.F., Weber, E.J., 2003. Reductive dehalogenation of halomethanes in iron- and sulfate-reducing sediments. 1. Reactivity pattern analysis. Environ. Sci. Technol. 37, 713–720. doi:10.1021/es0205941
- Klausen, J., Troeber, S.P., Haderlein, S.B., Schwarzenbach, R.P., 1995. Reduction of substituted nitrobenzenes by Fe(II) in aqueous mineral suspensions. Environ. Sci. Technol. 29, 2396–2404. doi:10.1021/es00009a036
- Kriegman-King, M.R., Reinhard, M., 1994. Transformation of carbon tetrachloride by pyrite in aqueous solution. Environ. Sci. Technol. 28, 692–700. doi:10.1021/es00053a025
- Kuder, T., Van Breukelen, B.M., Vanderford, M., Philp, P., 2013. 3D-CSIA: Carbon, chlorine, and hydrogen isotope fractionation in transformation of TCE to ethene by a *Dehalococcoides* culture. Environ. Sci. Technol. 47, 9668–9677. doi:10.1021/es400463p
- Lee, M., Wells, E., Wong, Y.K., Koenig, J., Adrian, L., Richnow, H.H., Manefield, M., 2015. Relative contributions of *Dehalobacter* and zerovalent iron in the degradation of chlorinated methanes. Environ. Sci. Technol. 49, 4481–4489. doi:10.1021/es5052364
- Liang, X., Butler, E.C., 2010. Effects of natural organic matter model compounds on the transformation of carbon tetrachloride by chloride green rust. Water Res. 44, 2125–2132. doi:10.1016/j.watres.2009.12.026
- Liang, X., Dong, Y., Kuder, T., Krumholz, L.R., Philp, R.P., Butler, E.C., 2007. Distinguishing abiotic and biotic transformation of tetrachloroethylene and trichloroethylene by stable carbon isotope fractionation. Environ. Sci. Technol. 41, 7094–7100. doi:10.1021/es070970n
- Lien, H.L., Zhang, W.X., 1999. Transformation of chlorinated methanes by nanoscale iron particles. J. Environ. Eng. 125, 1042–1047. doi:10.1061/(ASCE)0733-9372(1999)125:11(1042)
- Liger, E., Charlet, L., van Cappellen, P., 1999. Surface catalysis of uranium(VI) reduction by iron(II). Geochim. Cosmochim. Acta 63, 2939–2955. doi:10.1016/S0016-7037(99)00265-3
- Lin, Y.T., Liang, C., 2013. Carbon tetrachloride degradation by alkaline ascorbic acid solution. Environ. Sci. Technol. 47, 3299–3307. doi:10.1021/es304441e
- Lipczynska-Kochany, E., Harms, S., Milbum, R., Sprah, G., Nadarajah, N., 1994. Degradation of carbon tetrachloride in the presence of iron and sulphur containing compounds. Chemosphere 29, 1477–1489.
- Lojkasek-Lima, P., Aravena, R., Shouakar-Stash, O., Frape, S.K., Marchesi, M., Fiorenza, S., Vogan, J., 2012. Evaluating TCE abiotic and biotic degradation pathways in a permeable reactive barrier using compound specific isotope analysis. Ground Water Monit. Remediat. 32, 53–62. doi:10.1111/j1745
- Maithreepala, R.A., Doong, R., 2007. Dechlorination of carbon tetrachloride by ferrous ion associated with iron oxide nano particles, in: Proceedings of the Fourth Academic Sessions 2007.

- Matheson, L.J., Tratnyek, P.G., 1994. Reductive dehalogenation of chlorinated methanes by iron metal. Environ. Sci. Technol. 28, 2045–2053. doi:10.1021/es00061a012
- McCormick, M.L., Bouwer, E.J., Adriaens, P., 2002. Carbon tetrachloride transformation in a model iron-reducing culture: Relative kinetics of biotic and abiotic reactions. Environ. Sci. Technol. 36, 403–410. doi:10.1021/es010923+
- Neumann, A., Hofstetter, T.B., Skarpeli-Liati, M., Schwarzenbach, R.P., 2009. Reduction of polychlorinated ethanes and carbon tetrachloride by structural Fe(II) in smectites. Environ. Sci. Technol. 43, 4082–4089. doi:10.1021/es9001967
- Noubactep, C., 2009. On the validity of specific rate constants (k_{SA}) in Fe⁰/H₂O systems. J. Hazard. Mater. 164, 835–837. doi:10.1016/j.jhazmat.2008.08.074
- Palau, J., Shouakar-Stash, O., Hunkeler, D., 2014. Carbon and chlorine isotope analysis to identify abiotic degradation pathways of 1,1,1-trichloroethane. Environ. Sci. Technol. 48, 14400–14408. doi:10.1021/es504252z
- Puigdomènech, I., 2010. MEDUSA (Make Equilibrium Diagrams Using Sophisticated Algorithms) Windows interface to the MS-DOS versions of INPUT, SED and PREDOM (FORTRAN programs drawing chemical equilibrium diagrams).
- Renpenning, J., Keller, S., Cretnik, S., Shouakar-stash, O., Elsner, M., Schubert, T., Nijenhuis, I., 2014. Combined C and Cl isotope effects indicate differences between corrinoids and enzyme (*Sulfurospirillum multivorans* PceA) in reductive dehalogenation of tetrachloroethene, but not trichloroethene. Environ. Sci. Technol 48, 11837–11845. doi:dx.doi.org/10.1021/es503306g
- Rodríguez-Fernández, D., Torrentó, C., Guivernau, M., Viñas, M., Hunkeler, D., Soler, A., Domènech, C., Rosell, M., 2018. Vitamin B₁₂ effects on chlorinated methanes-degrading microcosms: Dual isotope and metabolically active microbial populations assessment. Sci. Total Environ. 621, 1615–1625. doi:10.1016/j.scitotenv.2017.10.067
- Sherwood Lollar, B., Hirschorn, S., Mundle, S.O.C., Grostern, A., Edwards, E.A., Lacrampe-Couloume, G., 2010. Insights into enzyme kinetics of chloroethane biodegradation using compound specific stable isotopes. Environ. Sci. Technol. 44, 7498–7503. doi:10.1021/es101330r
- Slater, G.F., Sherdwood Lollar, B., Lesage, S., Brown, S., 2003. Carbon isotope fractionation of PCE and TCE during dechlorination by vitamin B₁₂. Ground Water Monit. Remediat. 23, 59–67. doi:10.1111/j.1745-6592.2003.tb00695.x
- Slater, G.F., Sherwood Lollar, B., Allen King, R., O'Hannesin, S., 2002. Isotopic fractionation during reductive dechlorination of trichloroethene by zero-valent iron: influence of surface treatment. Chemosphere 49, 587–596. doi:10.1016/S0045-6535(02)00327-2
- Slater, G.F., Sherwood Lollar, B., Sleep, B.E., Edwards, E.A., 2001. Variability in carbon isotopic fractionation during biodegradation of chlorinated ethenes: Implications for field applications. Environ. Sci. Technol. 35, 901–907. doi:10.1021/es001583f
- Song, H., Carraway, E.R., 2006. Reduction of chlorinated methanes by nano-sized zero-valent iron. Kinetics, pathways and effect of reaction conditions. Environ. Eng. Sci. 23, 272–284. doi:10.1089/ees.2006.23.272
- Staudinger, J., Roberts, P. V., 2001. A critical compilation of Henry's law constant temperature dependence relations for organic compounds in dilute aqueous solutions. Chemosphere 44, 561–576. doi:10.1016/S0045-6535(00)00505-1

- Támara, M.L., Butler, E.C., 2004. Effects of iron purity and groundwater characteristics on rates and products in the degradation of carbon tetrachloride by iron metal. Environ. Sci. Technol. 38, 1866–1876. doi:10.1021/es0305508
- Torrentó, C., Palau, J., Rodríguez-Fernández, D., Heckel, B., Meyer, A., Domènech, C., Rosell, M., Soler, A., Elsner, M., Hunkeler, D., 2017. Carbon and chlorine isotope fractionation patterns associated with different engineered chloroform transformation reactions. Environ. Sci. Technol. 51, 6174–6184. doi:10.1021/acs.est.7b00679
- Van Breukelen, B.M., 2007. Extending the Rayleigh equation to allow competing isotope fractionating pathways to improve quantification of biodegradation. Environ. Sci. Technol. 41, 4004–4010. doi:10.1021/es0628452
- Vanstone, N., Elsner, M., Lacrampe-Couloume, G., Mabury, S., Sherwood Lollar, B., 2008. Potential for identifying abiotic chloroalkane degradation mechanisms using carbon isotopic fractionation. Environ. Sci. Technol. 42, 126–132. doi:10.1021/es0711819
- Vikesland, P.J., Heathcock, A.M., Rebodos, R.L., Makus, K.E., 2007. Particle size and aggregation effects on magnetite reactivity toward carbon tetrachloride. Environ. Sci. Technol. 41, 5277–5283. doi:10.1021/es062082i
- Wiegert, C., Aeppli, C., Knowles, T., Holmstrand, H., Evershed, R., Pancost, R.D., Macháčková, J., Gustafsson, Ö., 2012. Dual carbon-chlorine stable isotope investigation of sources and fate of chlorinated ethenes in contaminated groundwater. Environ. Sci. Technol. 46, 10918–10925. doi:10.1021/es3016843
- Wiegert, C., Mandalakis, M., Knowles, T., Polymenakou, P.N., Aeppli, C., Macháčková, J., Holmstrand, H., Evershed, R.P., Pancost, R.D., Gustafsson, O., 2013. Carbon and chlorine isotope fractionation during microbial degradation of tetra- and trichloroethene. Environ. Sci. Technol. 47, 6449–6456. doi:10.1021/es305236y
- World Health Organization, 2003. Iron in drinking-water. WHO Guidelines for drinking-water quality, WHO/SDE/WSH/03.04/08. Geneva.
- Zhang, X., Deng, B., Guo, J., Wang, Y., Lan, Y., 2011. Ligand-assisted degradation of carbon tetrachloride by microscale zero-valent iron. J. Environ. Manage. 92, 1328–1333. doi:10.1016/j.jenvman.2010.12.020
- Zwank, L., Elsner, M., Aeberhard, A., Schwarzenbach, R.P., 2005. Carbon isotope fractionation in the reductive dehalogenation of carbon tetrachloride at iron (hydr)oxide and iron sulfide minerals. Environ. Sci. Technol. 39, 5634–5641. doi:10.1021/es0487776